Eur. Phys. J. B **46**, 475–480 (2005)
DOI: 10.1140/epjb/e2005-00283-3

THE EUROPEAN PHYSICAL JOURNAL B

Hysteresis in small arrays of interacting magnetic nanoparticles

C. Xu[1,3,a], P.M. Hui[2], L.F. Zhang[1], Y.Q. Ma[3], J.H. Zhou[1], and Z.Y. Li[1]

[1] Department of Physics, Suzhou University, Suzhou 215006, P.R. China
[2] Department of Physics, The Chinese University of Hong Kong, Shatin, New Territories, Hong Kong, P.R. China
[3] National Laboratory of Solid State Microstructures, Nanjing University, Nanjing 210093, P.R. China

Received 28 April 2005 / Received in final form 31 May 2005
Published online 7 September 2005 –

Abstract. The out-of-plane hysteresis loops of small arrays of magnetic nanoparticles, under the influence of an external field applied perpendicular to the array and the dipolar interaction are investigated. The particles are assumed to have a perpendicular anisotropy energy that tends to align the magnetic moments to be perpendicular to the array. The magnetization is found to exhibit a plateaux-and-jumps structure as the external field is swept up and down. These jumps are associated with jumps in the energy of the system, and correspond to transition from one configuration of the moment orientation to another. The energy of different configurations of the magnetic moments for a 3×3 array in the limit of weak dipolar interaction is analyzed, as a means to understand the hysteresis loop. These jumps are more pronounced in arrays of smaller sizes and when the dipolar interaction is weak. The configuration of magnetic moments at zero external field as the field is swept up and down is found to be highly sensitive to the dipolar interaction.

PACS. 75.60.Ej Magnetization curves, hysteresis, Barkhausen and related effects – 75.60.Jk Magnetization reversal mechanisms – 75.75.+a Magnetic properties of nanostructures

1 Introduction

Arrays of single-domain magnetic dots are of substantial current research interest due to their potential applications in future ultrahigh-density magnetic storage media and magnetic field sensors [1–7]. In these systems, each nanoparticle or dot may be regarded as a giant magnetic dipole. In patterned arrays, the dipolar field may be comparable to the bulk anisotropy field due to high packing density of the particles and it may strongly affect static magnetic ordering and magnetization processes. Understanding the magnetic properties in such systems is, therefore, essential to the design of devices.

Of particular interest is the magnetization process in finite and small arrays. Kayali et al. [8] and Stamps et al. [9,10] found that magnetic ordering and hysteresis are strongly affected by the array size and the direction of the external applied field in a finite array of particles with magnetic moments constrained to be parallel to the array. Experimentally, Ross et al. [4], for example, studied patterned arrays of cylindrical nanoparticles of large aspect (height/diameter) ratio. These particles exhibit single-domain behavior and their easy axes are aligned perpendicular to the substrate surface, as a result of both shape anisotropy and magnetocrystalline anisotropy. For the weak dipolar interaction regime studied in their experiments, these particles have their moments pointed either "up" or "down", with respect to the direction perpendicular to the array. The strength of dipolar interaction is related to the separation between the magnetic particles and the relative orientations of the interacting magnetic moments. Therefore, a finite array of magnetic dots with magnetic moments not restricted to lie parallel to the plane of the array due to possibly large perpendicular anisotropy is expected to exhibit different properties from an array consisting only of in-plane magnetic moments [8]. In particular, the effects of dipolar interaction would be important in high-density patterned arrays. Fabrication of arrays of magnetic dots with controllable anisotropy thus opens up a further possibility in arriving at desirable magnetic properties.

In the present work, we study the hysteresis of an interacting array of nanoparticles with magnetic moments free to point at any direction in three-dimensional space under the influence of a perpendicular anisotropy energy and an external field applied perpendicular to the array. Our study is thus a generalization of the recent work of Kayali et al. [8] on in-plane hysteresis. Each particle is assumed to have a large perpendicular anisotropy, and the magnetic dipolar interaction between all particles in the array is taken into account. It is found that the magnetic properties of small arrays are highly sensitive to the strength of dipolar interaction and the size of the array. The magnetization exhibits a plateaux-and-jumps structure as the external field is swept up and down. These

[a] e-mail: cxu@suda.edu.cn

jumps are associated with jumps in the energy of the system, and correspond to transition from one configuration of the moment orientation to another. We analyze the energy of different configurations for a 3×3 array in the limit of weak dipolar interaction. The configuration of magnetic moments at zero external field as the field is swept up and down is found to be highly sensitive to the dipolar interaction.

2 Model of calculation

The hysteresis in an array of coupled magnetic moments can be studied via the Landau-Lifshitz-Gilbert (LLG) equation, which is an equation of motion for each of the moments. We consider a square array of identical magnetic dots. Each dot is treated as a single-domain particle with an effective magnetic moment $\mathbf{m}$. The ith dot is located at $\mathbf{r}_i = pa\hat{x} + qa\hat{y}$, where a is the lattice constant and p and q are integers. The equation of motion of the ith magnetic moment can be described by the LLG equation [11] as

$$\frac{d\mathbf{m}_i}{dt} = -\gamma \mathbf{m}_i \times \mathbf{H}_i + \frac{\alpha}{m}\mathbf{m}_i \times \frac{d\mathbf{m}_i}{dt} \ , \tag{1}$$

where γ is the gyromagnetic ratio and α represents the rate of dissipation. The local magnetic field $\mathbf{H}_i$ at site $\mathbf{r}_i$ includes various contributions:

$$\mathbf{H}_i = \mathbf{h}_e + \mathbf{h}_{dip} + km_{zi}\hat{z} \ , \tag{2}$$

where $\mathbf{h}_e$ is an external magnetic field, and $km_{zi}\hat{z} = (2K/M_s)m_{zi}\hat{z}$ is the single-particle effective anisotropy field perpendicular to the array [11] with K being the anisotropy energy and M_s the saturated magnetization of the particle. The dipolar field $\mathbf{h}_{dip}$ acting on the ith moment can be expressed as

$$\mathbf{h}_{dip} = \sum_{j \neq i} \left[\frac{3(\mathbf{r}_{ij} \cdot \mathbf{m}_j)\mathbf{r}_{ij}}{r_{ij}^5} - \frac{\mathbf{m}_j}{r_{ij}^3} \right] \ , \tag{3}$$

where the sum is over all the other particles in the array.

Assuming that $|\mathbf{m}_i| = m$ for all particles, the ith moment can then be fully specified by the angles (θ_i, ϕ_i) describing the orientation of $\mathbf{m}_i$, where θ is the polar angle measured from the normal ($\hat{z}$-direction) and ϕ is the azimuthal angle as defined in the spherical coordinates. It is convenient to define $t' = tM_s\gamma\left(1+\alpha^2\right)^{-1}$ and to measure time in units of t'. It follows from equation (1) that the orientation of $\mathbf{m}_i$ evolves in time as [12]

$$\frac{d\theta_i}{dt'} = -\sin\phi_i \frac{H_{ix}}{M_s} + \cos\phi_i \frac{H_{iy}}{M_s} + \alpha \left[\cos\theta_i \cos\phi_i \frac{H_{ix}}{M_s} + \cos\theta_i \sin\phi_i \frac{H_{iy}}{M_s} - \sin\theta_i \frac{H_{iz}}{M_s} \right] \ , \tag{4}$$

$$\frac{d\phi_i}{dt'} = -\frac{\cos\theta_i \cos\phi_i}{\sin\theta_i}\frac{H_{ix}}{M_s} - \frac{\cos\theta_i \sin\phi_i}{\sin\theta_i}\frac{H_{iy}}{M_s} + \frac{H_{iz}}{M_s} - \alpha \left[\frac{\sin\phi_i}{\sin\theta_i}\frac{H_{ix}}{M_s} - \frac{\cos\phi_i}{\sin\theta_i}\frac{H_{iy}}{M_s} \right] \ , \tag{5}$$

where H_{ix}, H_{iy}, H_{iz} are the Cartesian components of $\mathbf{H}_i$.

It is convenient to normalize the magnetization and fields by the magnetization in a dot M_s and to measure separations in units of the lattice constant a. The dipolar field can then be rewritten in a reduced form

$$\frac{\mathbf{h}_{dip}}{M_s} = h_d \sum_{j \neq i} \frac{3(\hat{\mathbf{r}}_{ij} \cdot \hat{\mathbf{m}}_j)\hat{\mathbf{r}}_{ij} - \hat{\mathbf{m}}_j}{\tilde{r}_{ij}^3} \ , \tag{6}$$

where $\hat{\mathbf{r}}_{ij}$ is a unit vector pointing from the dipole moment $\mathbf{m}_i$ to $\mathbf{m}_j$, $\mathbf{m}_j = m\hat{\mathbf{m}}_j$, and $\tilde{r}_{ij} = r_{ij}/a$. The dipolar interaction strength is then represented by the parameter h_d given by

$$h_d = \frac{m}{a^3 M_s} = \frac{V}{a^3} \ , \tag{7}$$

where V is the volume of a dot. Obviously, h_d increases as the volume of the particles increases with a fixed lattice constant.

We study the hysteresis loops for square arrays of size $N \times N$ with $N = 3, ..., 10$ subject to an external magnetic field applied perpendicular to the array, by solving equations (4–5) numerically using the fourth-order Runge-Kutta method. We sweep the external field $\mathbf{h}_e = h_e\hat{z}$, starting with a strong field $h_e = +H_0$ for which all the moments are aligned along the $+\hat{z}$-direction. The field strength h_e is then gradually decreased in increments of δh to $-H_0$, followed by an increase back to $+H_0$. At each value of h_e, equations (4 and 5) are solved for the orientations of the moments in the long time limit. This amounts to solving $2N^2$ coupled equations for an $N \times N$ array. To study the hysteresis loop, we use the steady state configuration obtained for the field $h_e \pm \delta h$ as the initial configuration for solving the equations for the field h_e when we sweep the field down and up. We apply a very small transverse bias field h_b ($h_b/k = 10^{-6}$) in the $\hat{x}$-direction to destabilize the initial configurations with all the moments pointing upwards so that the steady state can be achieved more readily [13]. We have checked that the small bias field h_b would not affect the steady state magnetic configurations. To further accelerate our calculations, we use a rather large damping constant ($\alpha = 1.0$). The choice of α, while affecting the time to reach the steady state, does not affect the final steady state configuration of the magnetic moments. In addition, we assume a large positive reduced anisotropic field $k/M_s = 2.0$ perpendicular to the array for the particles, as a model of single-domain particles in which there are both shape anisotropy (e.g., in cylindrical particles with large aspect ratios) and magnetocrystalline anisotropy.

3 Results and discussion

Figure 1 shows the $\hat{z}$-component of the magnetization M_z in a 3×3 array as a function of the applied field for several values of h_d representing different dipolar interaction strengths. The magnetization is normalized by the saturation magnetization M_0 of the array. Note that for widely separated particles (or negligible h_d) where the particles

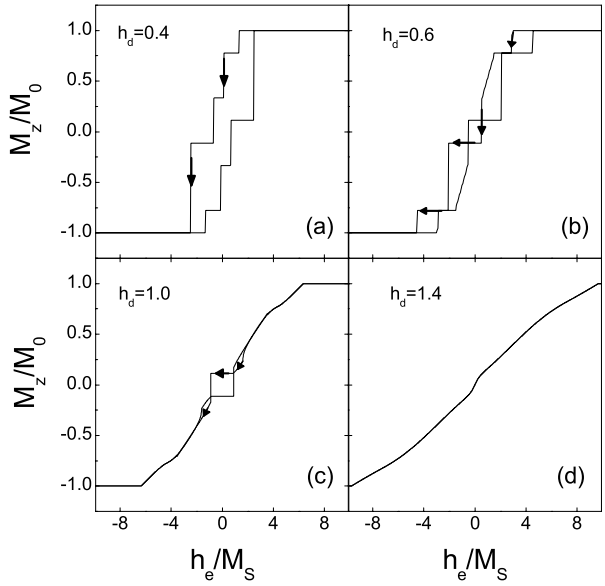

Fig. 1. Hysteresis loops for a 3×3 array of magnetic nanoparticles for different values of the dipolar interaction strength h_d. (a) $h_d = 0.4$, (b) $h_d = 0.6$, (c) $h_d = 1.0$, (d) $h_d = 1.4$.

become effectively isolated, the hysteresis loop is expected to take on a squared shape [6,14] as a result of the perpendicular anisotropy. Here we explore how the magnetization processes in a small array may depend on the dipolar interaction. When the dipolar interaction is weak (see Figs. 1a and 1b), the magnetization exhibits abrupt jumps. These jumps exist both for decreasing and increasing fields, but the values of h_e at which the jumps occur are different in these two cases. These jumps are caused by the effects of the strong perpendicular anisotropy, the dipolar interaction and the Zeeman energy. Due to the strong anisotropy, the moments preferentially tend to align perpendicular to the array, either along the $+\hat{z}$ or the $-\hat{z}$ direction. The dipolar interaction tends to align the neighboring moments to be anti-parallel to each other. With these two factors, the steady states still have the moments aligned normal to the array. As the external field decreases, the number of moments aligned with the $-\hat{z}$-direction gradually increases. The jumps comes about from energetic consideration. Since the anisotropy lowers the energy of the moments when they are aligned perpendicularly to the array, configurations with the moments pointing at any polar angles other than $\theta \approx 0$ and $\theta \approx \pi$ are of higher energies. Thus, for a moment to flip from the $+\hat{z}$-direction to the $-\hat{z}$ direction, it needs to pass through an energy barrier. Only when the external field reaches a certain value will the energy barrier be surpassed with the assistance of the Zeeman energy [15]. This leads to the plateaux-and-jumps structure in the magnetization shown in Figures 1a and 1b. These energy barriers are sensitive to the orientations of all the moments, and the magnitude of the external field for the jumps to occur depends on whether the field is decreasing or increasing. For example, the first jump for $h_d = 0.4$ as the external field decreases corresponds to the flipping of the moment at the center of the 3×3 array, as it is the most energetically favorable for the dipolar interaction. For stronger dipolar interaction (see Figs. 1c and 1d), the anisotropy no longer locks the moments to be normal to the array. The steady state configuration corresponds to one with moments pointing at some angles from the $\hat{z}$-direction. A stronger h_e is therefore needed to align all the moments to be up or down to achieve saturation. The dependence of the field needed for saturation on the dipolar interaction strength will be discussed later. The steps in the magnetization become less apparent. For very strong dipolar interaction, the moments prefer to align parallel to the array, with an antiferromagnetic in-plane alignment. This gives rise to the vanishing M_z in the absence of an external field $h_e = 0$ in Figure 1d.

It may be surprising to see the magnetization curves in Figures 1b and 1c cross each other as the field is swept down and up. It should be noted that similar feature has been reported in other systems of small sizes [8,9]. Note that the part of the magnetization curve for decreasing external field is identical to the part for increasing external field, as required by symmetry. The crossing comes about from the sensitive dependence on history in small arrays. As discussed in the previous section, when the field is swept down gradually, the initial configuration of the magnetic moments for the calculation at the external field $h_e - \delta h$ is taken to be the steady state configuration obtained at the field h_e by solving the LLG equations for the array. In doing so, the resulting configuration is highly sensitive to the local energy barrier separating the configuration at h_e and possible configurations corresponding to $h_e - \delta h$. The plateaux-and-jumps features in the magnetization curve come from the non-trivial transitions between allowed energies. These transitions, as the field is swept down or up, can be viewed as a path in the complicated energy landscape produced by the external field, anisotropy and dipolar interaction. It turns out that these transitions often do not go into the state of lowest possible energy for given external field and dipolar interaction strength, as will be discussed in Figure 2.

It is illustrative to trace the energy of the system shown in Figure 1a as the external field decreases. As the field decreases, the system passes through different configurations of the moments. Accompanied with each of these configurations is an energy of the system. The energy E is formally given by

$$\frac{E}{M_s m} = -\frac{1}{2}\sum_i \hat{\mathbf{m}}_i \cdot \frac{\mathbf{h}_{dip}}{M_s} + \frac{1}{2}\sum_i \frac{k}{M_s}\sin^2(\mathbf{m}_i, \hat{z}) - \sum_i \hat{\mathbf{m}}_i \cdot \frac{\mathbf{h}_e}{M_s}, \tag{8}$$

where the argument in the sine function is the angle between the magnetic moment and the $\hat{z}$-axis. For the case of weak dipolar interaction ($h_d = 0.4$) studied here, the second term with the sine function can be neglected, as the magnetic moments are aligned perpendicular to the array by the dominating anisotropy energy. Figure 2a shows the energy as the external field is reduced. The inset

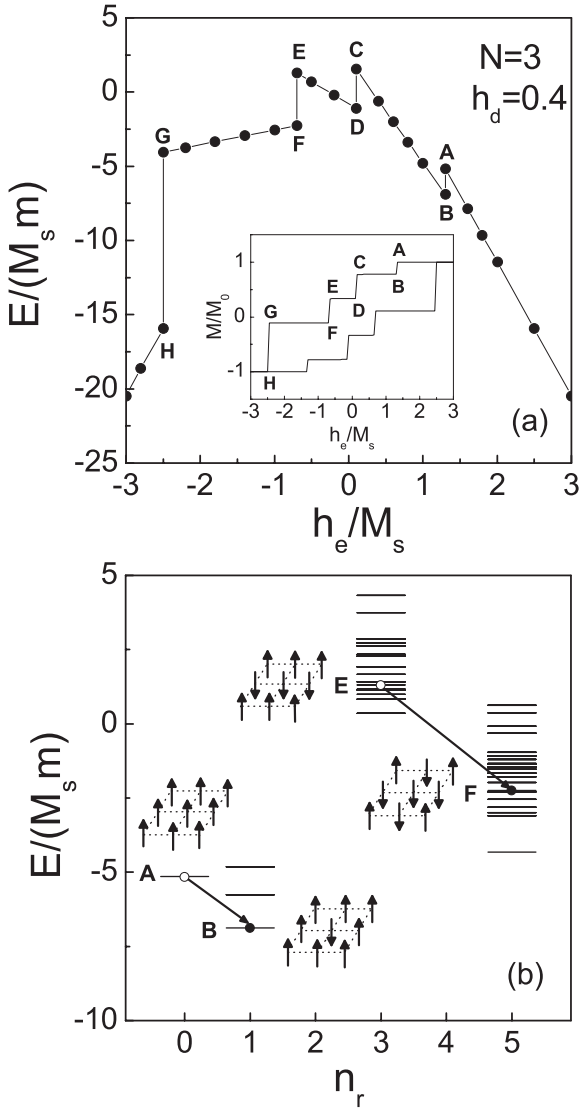

Fig. 2. (a) The energy $E/(M_s m)$ of a 3×3 array as a function of a decreasing external field h_e for a fixed dipolar interaction strength of $h_d = 0.4$. The inset shows the magnetization loop. The labels A to H give the jumps in the magnetization (inset) and the corresponding jumps in energy. (b) The possible energies for a system with at a given number of flipped moment n_r, when the moments are restricted to be perpendicular to the array. The transition from A ($n_r = 0$) to B ($n_r = 1$) and from E ($n_r = 3$) to F ($n_r = 5$) are shown. The open circles give the energy of the configuration at A and E and the closed circles give the energy at B and F. Also shown are the configurations of the magnetic moments corresponding to the point A, B, E, and F.

reproduces the hysteresis (as shown in Fig. 1a) as guide to the eye. The labels A to H in the figure and the inset mark the jumps in the magnetization and the corresponding jumps in the energy of the system.

To further illustrate the nature of the changes in the orientation of the moments, we focus on the changes labelled A to B and E to F in Figure 2a. Decreasing from very strong external field, the energy of the system increases as the Zeeman energy becomes less negative, until the system reaches the point labelled A (see Fig. 2a), where the moments are all pointing in the $+\hat{z}$-direction (as shown in Fig. 2b). At this field, the magnetic moment at the center of the array flips. Note that even with the simplification of restricting the moments to be aligned perpendicular to the array, the energy of a system with one moment flipped can take on several possible energies, as the flipped moment can be any one of the moments. Using equation (8), it is possible to calculate the energy of all the possible configurations corresponding to one flipped moment. The results are shown in Figure 2b at $n_r = 1$, where n_r is the number of moments flipped to the $-\hat{z}$-direction. There are three possible energies, corresponding to the flipping of the moment at the center (one possible configuration), the moment in the middle of an edge (four possible equivalent configurations), and the moment at the four corners (four possible equivalent configurations). Thus, the nine configurations with one flipped moments take on only three possible energies, with a non-degenerate lowest energy and two higher energies of four-fold degeneracy. The transition from A to B turns out to be a transition to the configuration with the flipped moment at the center of the array. The selection of the resulting configuration does not only depend on the energy of the configuration, but also the energy barrier between the initial and the final configurations. This, in turn, is controlled by a combination of the anisotropy energy, dipole interaction and the Zeeman energy. The configuration as the field decreases to $h_e = 0$ is characterized by the flipping of a row of moments in the middle of the array (see configuration labelled E in Fig. 2b). The configuration has a net number of moments in the $+\hat{z}$-direction, and thus one could associate a positive remanence to the array in this case. Note that there are many configurations with three flipped moments that give the same magnetization. The energies of these configurations are shown in Figure 2b at $n_r = 3$. The configuration E is marked by the open circle. The transition to F corresponds to a change in configuration to one that has five flipped moments (labelled F). There are, again, many configurations with different energies corresponding to five flipped moments in the array. The one corresponding to F is marked by a closed circle. Here the transition from E to F, while leads to a drop in energy, does not go to the lowest possible energy that the value of the magnetization allows. The energy barriers from E to each of the possible energies with $n_r = 5$ are different, and the external field at the transition assists to surpass the barrier from E to F.

We define the remanence M_r of an array as the $\hat{z}$-component of the magnetization at $h_e = 0$ for a decreasing field. We have carried out calculations similar to that in Figure 2a for different values of h_d and found the configurations at $h_e = 0$. Figure 3 shows the values of M_r, together with the configurations for a decreasing field at $h_e = 0$, for different dipolar interaction strengths h_d in a 3×3 array. Note that as h_d increases, more magnetic moments are aligned anti-parallel to their neighboring moments to make use of the increasing dipolar interaction.

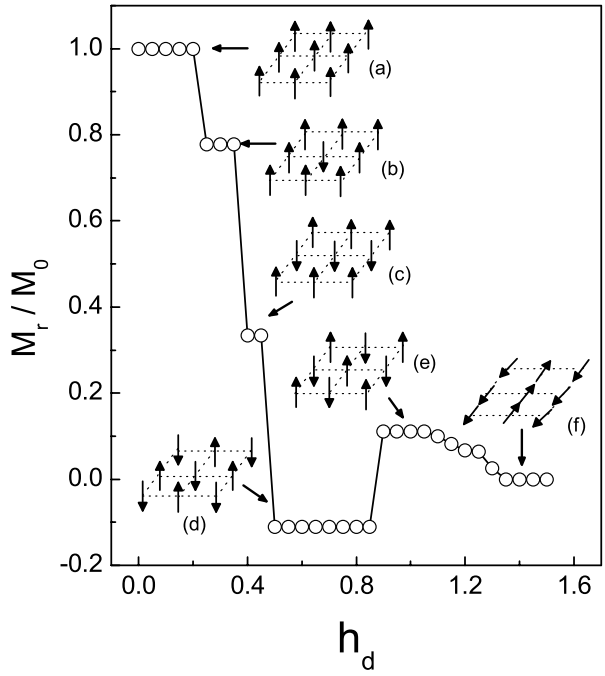

Fig. 3. The reduced remanence M_r/M_0 for a decreasing external field in a 3×3 array with different dipole interaction strengths. The sketches show the configurations of the magnetic moments at $h_e = 0$ for a decreasing field.

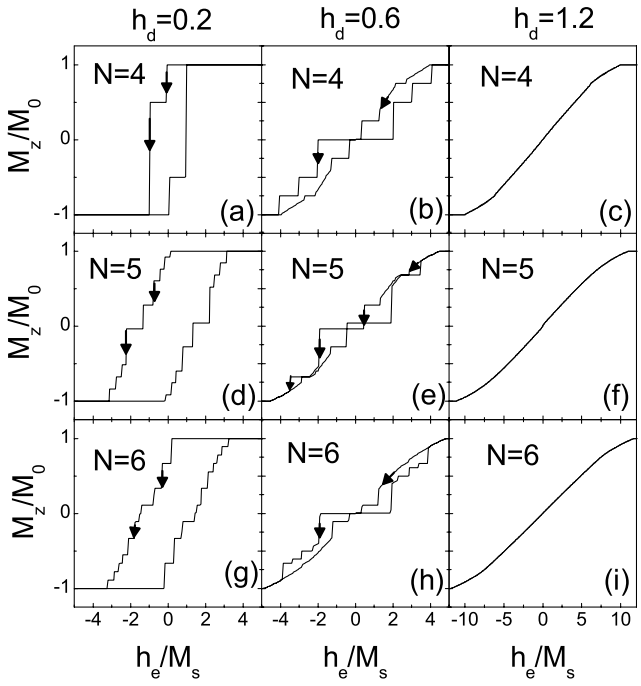

Fig. 4. Hysteresis loops for $N \times N$ arrays with $N = 4$, 5, and 6, for different dipolar interaction strengths h_d.

At high h_d, the moments take on an in-plane anti-parallel chain-like structure. The results show the high sensitivity of the configuration at $h_e = 0$ to the dipolar interaction strength.

Figure 4 shows the results of the magnetization as a function of the external field for 4×4, 5×5 and 6×6 arrays and different values of the dipolar interaction strengths. As the size increases, the jumps become less abrupt but occur more frequently. As mentioned, these jumps are results of a complicated energy landscape constructed by the different contributions to the total energy. As the system size increases, the number of configurations for a given magnetization rapidly increases. There are, therefore, more local minima in the energy but the energy barriers become less severe to overcome. This gives rise to the many small drops in M_z as the system size increases (see the figures for $h_d = 0.2$). Note that for small arrays, the ratio of the number of moments at the boundary to the total number of moments is high and the effective field on a moment at the boundary is quite different from that on a moment inside the array. This leads to the preferential switching of magnetic moments, e.g., the switching of the moment in the middle of a 3×3 array as shown in Figure 2. We have only studied square arrays in the present work. It will also be interesting to study arrays with different width and length, i.e., arrays with aspect ratios different from unity. Note that the remanence of an array when dipolar interaction cannot be neglected also depends on whether the array consists of an odd or even number of moments. In the absence of an external field, the moments tend to make use of both the anisotropy energy and the dipolar interaction. Only arrays with an even number of moments could possibly lead to a vanishing remanence. For larger h_d, there are again a rapid increase in the number of configurations as the moments are no longer restricted to be normal to the array. Thus the magnetization curve tends to look smoother and the hysteresis loop is smaller. For a dominating dipolar interaction ($h_d = 1.2$), there is no hysteresis loop as the moments are forced to take on an in-plane orientation. These features are also observed in arrays up to a size of 10×10.

Finally, as noted in the discussion on Figure 1, the minimum value of the external field $h_{e,sat}$ that leads to saturated magnetization in an array increases with h_d. Figure 5 shows the dependence of $h_{e,sat}$ on the size of the array N for different values of the dipolar interaction strength. Quite generally, size effects drop out for arrays with size 10×10 or larger, as the magnetic moments inside the array become dominating.

4 Summary

In summary, we studied the out-of-plane hysteresis loops of small arrays of magnetic nanoparticles, under the influence of a perpendicular anisotropy energy, an external field applied perpendicular to the array and the dipolar interaction. The magnetization exhibits a plateaux-and-jumps structure as the external field is swept up and down. These jumps are associated with jumps in the energy of the system, and correspond to transition from one configuration of the moment orientation to another. We analyzed the energy of different configurations for a 3×3 array in the

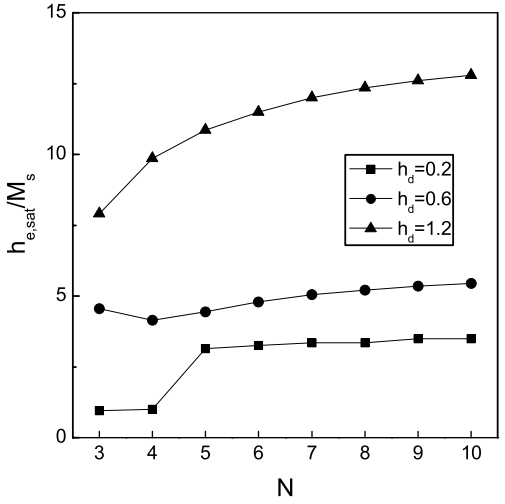

Fig. 5. The reduced external field $h_{e,sat}/M_s$ as a function of N for $h_d = 0.2$, 0.6, and 1.2.

limit of weak dipolar interaction. These jumps are more pronounced in arrays of smaller size and when the dipolar interaction is weak. The configuration of magnetic moments at vanishing external field as the field is swept up and down are found to be highly sensitive to the dipolar interaction. This sensitivity comes about from the formation of a complicated energy landscape in the parameter (phase) space constructed by the effects of the anisotropy, dipolar interaction, and the external field. While we have confined our studies to square arrays and to steady state configurations of magnetic moments, it would definitely be interesting to extend the present work to investigate the dependence of the magnetization processes on the different geometrical patterns of the array, e.g., triangular arrays, and the time that a system needs to approach the steady state.

References

1. *Magnetic Nanostructures* edited by H.S. Nalwa (American Scientific Publishers, 2002)
2. J.I. Martín, J. Nogués, K. Liu, J.L. Vicent, I.K. Schuller, J. Magn. Magn. Mater. **256**, 449 (2003)
3. J. Bai, H. Takahoshi, H. Ito, H. Satio, S. Ishio, J. Appl. Phys. **91**, 6848 (2004)
4. C.A. Ross, S. Haratani, F.J. Castaño, Y. Hao, M. Hwang, M. Shima, J. Y. Cheng, B. Vögeli, M. Farhoud, M. Walsh, H.I. Smith, J. Appl. Phys. **96**, 1133 (2002)
5. X. Zhu, P. Grütter, V. Metlushko, B. Ilic, Phys. Rev. B **66**, 024423 (2002)
6. C.A. Ross et al., Phys. Rev. B **65**, 144417 (2002)
7. S. Sun, C.B. Murray, D. Weller, L. Folks, A. Moser, Science **287**, 1989 (2000)
8. M. Amin Kayali, W.M. Saslow, Phys. Rev. B **70**, 174404 (2004)
9. R.L. Stamps, R.E. Camley, Phys. Rev. B **60**, 11694 (1999)
10. R.L. Stamps, R.E. Camley, J. Magn. Magn. Mater. **177–181**, 813 (1998)
11. R.L. Stamps, B. Hillebrands, Appl. Phys. Lett. **75**, 1143 (1999).
12. C. Xu, P.M. Hui, J.H. Zhou, Z.Y. Li, J. Appl. Phys. **91**, 5957 (2002)
13. R. L. Stamps, R.E. Camley, Phys. Rev. B **60**, 12264 (1999)
14. D. Grundler, G. Meier, K.-B. Broocks, Ch. Heyn, D. Heitmann, J. Appl. Phys. **85**, 6175 (1999)
15. L.F. Zhang, C. Xu, P.M. Hui, Y.Q. Ma, J. Appl. Phys. **97**, 103912 (2005)